Journal of Porphyrins and Phthalocyanines
J. Porphyrins Phthalocyanines 2019; **23**: 1–10
DOI: 10.1142/S1088424619500433

Published at http://www.worldscinet.com/jpp/

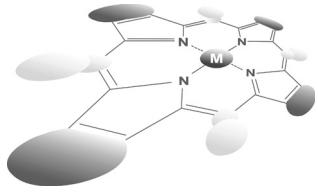

Synthesis, structure, photophysical, electrochemical properties and antibacterial activity of brominated BODIPYs as an inhibitor of DNA gyrase B of *S. aureus*

Dijo Prasannan[a], Chennakkandathil Sareena[b†], Chellaiah Arunkumar[a] and Suchithra Tharamel Vasu[b*]

[a] *Bioinorganic Materials Research Laboratory, Department of Chemistry, National Institute of Technology Calicut, NIT Campus, P.O., Calicut, India-673 601*
[b] *School of Biotechnology, National Institute of Technology Calicut, NIT Campus, P.O., Calicut, India-673 601*

Received 8 December 2018
Accepted 28 February 2019

ABSTRACT: BODIPYs with 3-thienyl and 4-acetamido phenyl groups substituted at the *meso*-position are subjected to regioselective bromination using three equivalents of *N*-bromosuccinimide (NBS) to yield their 2-mono and 2,6-di bromoderivatives. Their photophysical, electrochemical and antimicrobial properties are investigated. This paper presents a mechanistic investigation of the antibacterial effect of brominated BODIPYs, particularly against *Staphylococcus aureus*. Fluorescence microscopic images reveal that the compounds are internalized effectively within the bacterial cells, making it an ideal antibacterial drug. Morphological analysis of the bacterial cells after the treatment with the test compounds showed that the compounds did not affect the cell membrane or cell wall and the antibacterial effect of these compounds is achieved *via* a different mechanism. The most effective compound was selected to explore the target of action. Molecular docking studies were performed on 22 selected proteins in *S. aureus* and the *in silico* results were validated by *in vitro* experiments. It was observed that the supercoiling activity of DNA gyrase was completely inhibited by the 2,6-dibromo-1,3,5,7-tetramethyl-8-(4-acetamido)-4-bora-3a,4a-diaza-*s*-indacene, **3c** by forming H-bonds with the ASP 81 residue of the enzyme.

KEYWORDS: BODIPYs, DNA gyrase B, *Staphylococcus aureus*, antibacterial studies, docking, fluorescence imaging.

INTRODUCTION

Out of the numerous available flurophores such as rhodamine, fluorescein, phthalocyanine and squaraine, 4,4-difluoro-4-bora-3a,4a-diaza-s-indacene (BODIPYs) dyes with their superior photophysical properties and flexible functionalization nature have a distinctive position [1]. BODIPYs have become one of the cornerstones in biotechnology, due to their prospective applications in biomolecular labeling [2], medical diagnosis, drug delivery [3], cellular pH [4] and viscosity sensing [5]. Their high tissue penetration with minimal autofluorescence from biological samples makes them good candidates for use in biology. The biological properties of BODIPYs, particularly their antimicrobial and anticancer properties, have been well reported in literature [6–8]. BODIPYs featuring iodine atoms on the 2,6-positions used in *in vitro* photodynamic antimicrobial chemotherapy (PACT) have been proven to be effective against *S. xylosus* and *E. coli* under mild conditions [9]; antimicrobial activity of 2,6-diiodo-substituted

*Correspondence to: Suchithra Tharamel Vasu, School of Biotechnology, National Institute of Technology Calicut, NIT Campus P.O., Calicut, India-673 601, tel.: +91 (495) 2285318 (lab), +91 9744244461 (mobile), fax: +91 (495) 2287250, email: drtvsuchithra@nitc.ac.in

†Current address: [b]School of Biotechnology, National Institute of Technology Calicut, NIT Campus P.O., Calicut, India-673 601, tel.: +91 (495) 2285318 (lab), +91 9744244461 (mobile), fax: + 91 (495) 2287250.

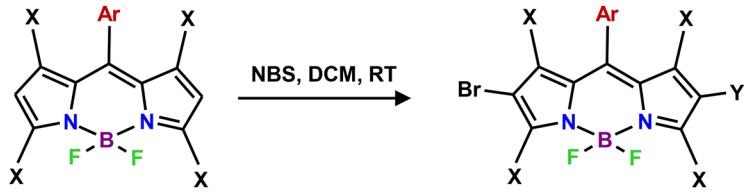

Ar = 3-thienyl; X = H; 1a
Ar = ph-4-NHCOCH$_3$; X = H; 2a
Ar = ph-4-NHCOCH$_3$; X = CH$_3$; 3a

Ar = 3-thienyl; X = Y = H; 1b, 30 %
Ar = 3-thienyl; X = H; Y = Br; 1c, 55 %
Ar = ph-4-NHCOCH$_3$; X = Y = H; 2b, 9 %
Ar = ph-4-NHCOCH$_3$; X = H; Y = Br; 2c, 18 %
Ar = ph-4-NHCOCH$_3$; X = CH$_3$; Y = H; 3b, 0 %
Ar = ph-4-NHCOCH$_3$; X = CH$_3$; Y = Br; 3c, 38 %

Scheme 1. Synthesis of brominated BODIPYs

BODIPY has been reported against *P. aeruginosa* [10]. Halogenated BODIPY dyes due, to their heavy atom effect, display efficient intersystem crossing (ISC) and act as photosensitizers to exhibit photocytotoxicity [11, 12]. Heavy atoms like bromine could induce triplet-state formation, and the generation of reactive singlet oxygen species has been the key cytotoxic agent in the therapeutic process, fostering cell death by an apoptotic and/or necrotic mechanisms [13]. Apart from this key cytotoxic mechanism, no other well-established therapeutic mechanism has been reported to foster cell death in presence of halogenated BODIPYs. Hence, it is very interesting to report here the bioactivity of brominated BODIPYs where the photosensitizing property is not responsible for their antibacterial properties.

The emergence of multidrug-resistant strains of pathogens demands strategies for developing antibacterial agents with novel mechanisms of action. Cellular microenvironments are complex, thus identifying the exact mode and target leading to intracellular toxicity is a topic of investigation. Among the different targets identified, DNA gyrase is a well-known pharmacological target for antibacterial drugs because it has not been found in eukaryotes. This prokaryotic type II topoisomerase consists of the subunits GyrA and GyrB, with different functional domains. The GyrA subunit is principally involved in DNA breakage and recombination of the supercoiling reaction, whereas the GyrB subunit is responsible for the ATP hydrolysis reaction. The derivatives of dibromopyrrolamides, including coumarin, thiophene, pyrazole and quinolone, are potent against gram-positive strains and are well established [14–17]. The rise of methicillin-resistant *Staphylococcus aureus* explains the current relevance of new classes of DNA gyrase inhibitors [18].

The present work focuses on the antibacterial activity of 2,6-dibromo BODIPYs with a representative member of gram-positive bacteria, *S. aureus*. As the electronic structure of a molecule has a key role in inducing toxicity, BODIPYs containing a thiophene ring and an amide group were selected for the study [19]. The antimicrobial activity of cationic BODIPY derivatives is well described [9, 20, 21]; hence the need for investigating the mechanism of bacterial cell disruption in uncharged BODIPY species is also necessary. Here, we explore the mechanism of action *via in silico* analysis, and this has been validated by *in vitro* studies. To the best of our knowledge, this paper reports for the very first time 2,6-dibromo BODIPY as a novel inhibitor of DNA gyrase of *S. aureus,* and we anticipate that the compound **3c** is a promising lead structure for various medical applications.

RESULTS AND DISCUSSION

The precursors, dipyrromethane and BODIPYs, were obtained in fairly good yield, 52–68% [13]. Bromination reactions were done according to procedures from the literature to afford 2,6-dibromo derivatives as the major product [13]. The overall synthetic route is outlined in Scheme 1. The structures were confirmed by IR, NMR spectroscopy and mass spectrometry, as presented in the Supplementary information, Figs S1 to S20. The B–F, B–N, and –C=N, of the BODIPY core were spotted as IR vibrations near 1532, 1400, and 1734 cm^{-1} respectively. The β–H of pyrrole ring [13], observed near 775 and 771 cm^{-1} in **1a** and **1c**, was absent in corresponding dibrominated product **1b**. The broad peak at 7.86 ppm and one proton singlet at 5.51 ppm respective of –NH and *meso*-proton in dipyrromethane **1** were absent in BODIPY **1a**. The absence of the two proton intensities respective of the β-pyrrole proton signals indicates successful dibromination at 2,6-pyrrolic position [13].

Photophysical properties

The photophysical properties of the synthesized BODIPY derivatives are summarized in Table 1. With increasing numbers of bromine atoms, a systematic bathochromic shift is observed in both absorption and emission profiles. The S_0–S_1 transition at 505 nm for compound **1a** in dichloromethane is red shifted by 13 nm with the incorporation of one bromine atom at β-positions; 518 nm

Table 1. Absorption and emission properties of compounds **1–2** (**a–c**), **3a** and **3c** in DCM, at λ_{ex} = 480 nm and slit width, 9. The molar extinction coefficient (ε) and fluorescence quantum yields (Φ_f) of compounds were calculated in toluene. Fluorescein in aqueous NaOH (0.1 N, Φ_f = 0.90) at λ_{ex} = 480 nm was used as the reference

Compound	λ_{abs} (nm)	λ_{em} (nm)	Φ_f	log ε	Maximum brightness $\Phi \times \varepsilon/10^3$ $M^{-1} \cdot cm^{-1}$	Singlet oxygen quantum yield (Φ_Δ)	Phototoxic power (PP)
1a	502	518	0.23	4.80	14.48	0.10	6310
1b	518	543	0.09	4.62	3.74	0.63	26 263
1c	543	567	0.04	4.32	0.75	0.26	5432
2a	502	516	0.05	4.58	1.82	0.12	4562
2b	518	548	0.07	4.78	1.63	0.64	38 564
2c	540	568	0.03	4.73	4.36	0.88	47 259
3a	502	510	0.42	4.76	24.58	0.10	5754
3c	529	542	0.13	4.96	12.48	0.97	88 465

for 2-mono-(**1c**) and 543 nm for 2,6-di-bromo (**1b**) derivative. The geometries of the ground state (S_0) and the first excited state (S_1) are similar; hence the emission spectrum of the BODIPY is the mirror image of the S_0 to S_1 of the dye. No notable solvatochromic effect was observed for absorption or emission with solvents of varying refractive indices, Table S1. Halogenated BODIPYs are well known for singlet oxygen production by heavy atom effects; the singlet oxygen quantum yield (Φ_Δ) computed are comparable to that of recent reports in the literature [22]. The singlet oxygen production in brominated BODIPYs is proven by diphenylisobenzofuran (DPBF) titration [13]. When DPBF is irradiated in the presence of BODIPYs, the singlet oxygen ($^1O_2$) species generated in the presence of BODIPYs deplete DPBF molecules and can be followed by measuring the decrease in absorbance of DPBF at 410 at regular irradiation intervals. The plot of absorbance *vs.* irradiation time reflects the singlet oxygen yield of the compounds as shown in Fig. S21. The phototoxic power (PP) of the BODIPY molecules are also shown in Table 1 [13, 23, 24]. As there are many factors contributing to the complete antimicrobial efficacy, a higher PP value alone does not guarantee effective antibacterial efficacy. Photo images and representative normalized optical and fluorescence (dash) profiles of BODIPYs, **1a**, **1b** and **1c** in toluene at room temperature are shown in the Supplementary information, Figs S22 and S23 respectively.

Electrochemical studies

Electrochemical studies were performed to analyze the effect of bromine groups on the BODIPY core, and the cyclic voltammograms of all BODIPYs show one reversible reduction and one irreversible reduction. A representative voltammogram of **1a–1c** is shown in Fig. 1. A successive anodic shift in the reduction wave potential is observed in all the series **1–2** (**a–c**), **3a** and **3c**, indicating that the BODIPY becomes easier to reduce

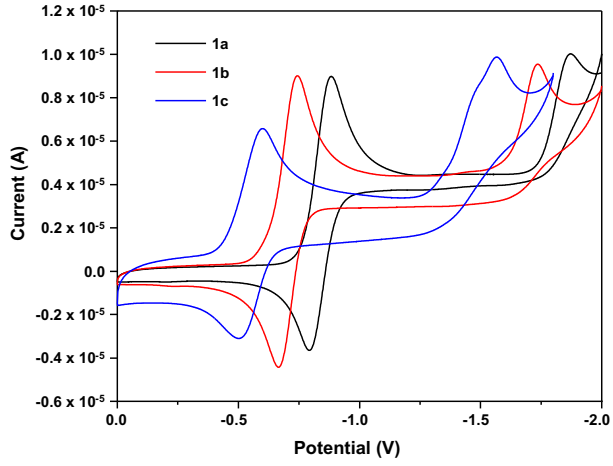

Fig. 1. Cyclic voltammogram of BODIPYs **1a–1c** in dichloromethane containing 0.1 M tetrabutylammonium hexafluoro phosphate as the supporting electrolyte at 100 mV/s

with the increase of the number of bromine atoms on the β-position [13] as shown in Table 2.

Single crystal X-ray diffraction studies

Compounds, **1b**, **2a**, **3a** and **3c**, crystallized in acetone/cyclohexane, chloroform/hexane and chloroform/cyclo hexane respectively, are characterized by X-ray crystal structure analyses and the data are presented in Table 3. Compound **3a** was crystallized in orthorhombic (**3a**·H_2O) and triclinic (**3a**·DMF·CH_3COOH) crystal systems with different solvent molecules in the crystal lattices. The molecular structures of compounds, **1b**, **2a**, **3a** and **3c** are shown in Fig. 2. The mono-bromo (**1b**) and di-bromo (**3c**) derivatives are well stabilized by two types of interactions, namely, $_{(thienyl)}$C···Br (3.448 Å), $_{(thienyl)}$H···F (2.479 Å) and $_{(phenyl)}$C···Br (3.451 Å) and $_{(phenyl)}$H···F (2.560 Å) respectively as shown in Figs 2a and 2e. Moreover, the existence of strong hydrogen

Table 2. Electrochemical data of dyes, **1a**–**3c**

Compound	Reduction potential (V)	
	I	**II**
1a	-0.84	-1.80
1b	-0.70	-1.68
1c	-0.55	-1.48
2a	-0.85	-1.83
2b	-0.75	-1.67
2c	-0.61	-1.54
3a	-1.25	-1.72
3c	-1.02	-1.84

bonding in two of the crystal structures of **3a** is one of the key factors for stabilizing the molecules (2.574 Å in **3a**·H_2O and 2.202 Å in **3a**·DMF·CH_3COOH). The interactions present in the crystals of **1b**, **2a**, **3a** and **3c** were quantified using *Crystal Explorer* 3.1. Hirshfeld surface analysis provides a 3D picture of close contacts present in the crystals which are summarized in a 2D fingerprint plot, Fig. S24. The H–H (23–51%), C–H (6.5–18%) and H–F (11.1–21%) interactions make the largest contribution to the Hirshfeld surfaces in each crystal, as presented in Fig. 3.

Antibacterial properties

All the compounds (1 mg/mL) were tested for antimicrobial activity against *S. aureus* under light and dark conditions, Table 4 [13]. The percentage zone of inhibition observed in agar well diffusion for **1c**, **2b**, **2c** and **3c** is promising and is comparable to that of the commercially available antibiotic vancomycin. Interestingly, the antibacterial activities were comparable under light and dark conditions, which clearly indicate that it is not the photosensitizing activity of brominated BODIPYs which is responsible for the antibacterial activity. Hence, further evaluation of antibacterial activity was done under ambient light conditions. The minimum inhibitory concentration (MIC) was determined using the broth dilution method in 96-well microtitre plates as well as a resazurin reduction assay [25, 26]. Both the assays showed same values of MIC, and the order is, **1b** ≈ **1c** > **2b** ≈ **2c** > **3c**; the highest being observed for unbrominated derivatives (**1a**, **2a** and **3a**), 100 μg/mL and the lowest, 20 μg/mL for **3c** as shown in Table 4. The presence of two bromine atoms and an amide group in the molecule may impart a synergistic effect to

Table 3. Crystal data and structure refinement parameters for compounds, **1b**, **2a**, **3a** and **3c**

Parameters	**1b**	**2a**	**3a**·H_2O	**3a**·DMF·CH_3COOH	**3c**
Molecular formula	$C_{13}H_8BBrF_2N_2S$	$C_{17}H_{14}BF_2N_3O$	$C_{21}H_{24}BF_2N_3O_2$	$C_{47}H_{55}B_2F_4N_7O_5$	$C_{21}H_{20}BBr_2F_2N_3O$
Formula weight	352.99	325.12	399.24	895.60	539.03
CCDC number	1577779	1022866	1033432	1058023	1577778
Temperature/K	293 (2)	296 (2)	296 (2)	293 (2)	293 (2)
Crystal system	Monoclinic	Triclinic	Orthorhombic	Monoclinic	Monoclinic
Space group	$P2_1/n$	P-1	$P2_12_12_1$	$P2_1/c$	$P2_1/n$
λ/Å	0.71073	0.71073	0.71073	0.71073	0.71073
a/Å	10.5117 (8)	9.6236 (4)	9.3409 (7)	10.7156 (14)	17.2407 (7)
b/Å	7.2016 (6)	13.0176 (5)	9.5069 (6)	45.965 (5)	7.8770 (4)
c/Å	17.4185 (15)	13.3553 (6)	23.1828 (17)	9.4560 (12)	17.4257 (9)
α (°)	90	109.777 (2)	90	90	90
β (°)	95.658 (3)	93.596 (2)	90	93.827 (3)	113.9710 (10)
γ (°)	90	95.930 (2)	90	90	90
Volume/Å^3	1312.17 (19)	1557.44 (11)	2058.7 (3)	4647.1 (10)	2162.39 (18)
Z	4	4	4	4	4
$Density_{calcd}$/mg m^{-3}	1.787	1.387	1.288	1.280	1.656
F (000)	696	672	840	1888	1072
θ range (°)	2.350 to 25.000	2.551 to 28.315	1.76 to 25.99	2.101 to 25.000	2.157 to 24.996
Data/parameters	2314/181	7442/436	4046/280	7902/676	3807/275
GOF on F^2	1.182	0.990	1.069	1.064	1.024
R_1[a], wR_2[b] [$I > 2\sigma$ (I)]	0.0421, 0.0995	0.0512, 0.1167	0.0330, 0.0810	0.0785, 0.1745	0.0331, 0.0794

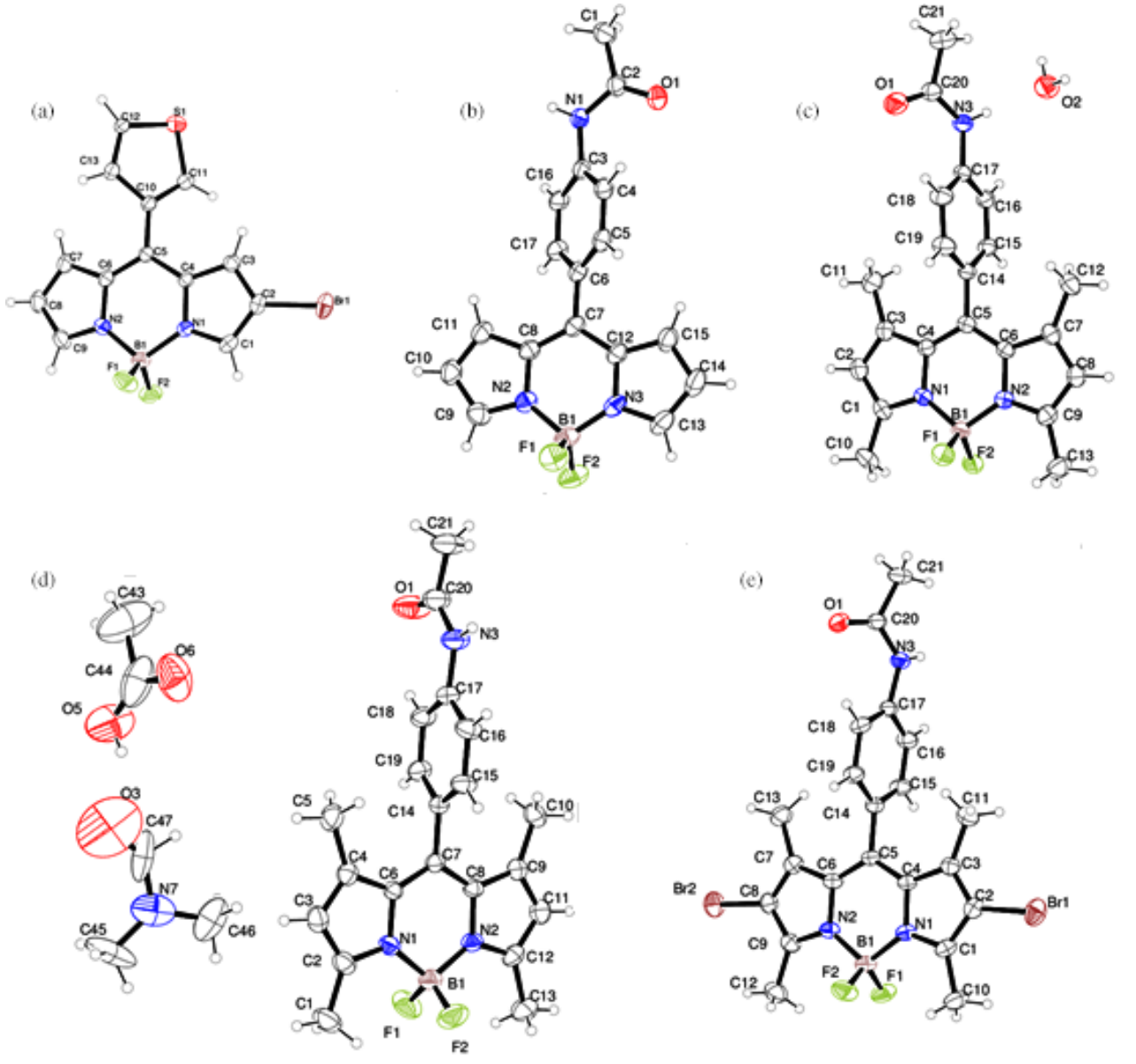

Fig. 2. Molecular structures (40% probability level) of (a) **1b**, (b) **2a**, (c) **3a**·H_2O, (d) **3a**·DMF·CH_3COOH and (e) **3c**

improve the antibacterial efficacy of the compound. This is reflected in the MIC value. The minimum bactericidal concentration (MBC) [27] values computed by time-kill assay also showed lower MBC values, 60–80 μg/mL for brominated derivatives. The brominated BODIPY derivative **3c** which shows fairly good MIC and MBC was chosen for further study.

The mode of action of BODIPY as antimicrobial photodynamic therapeutic agent is well reported [28]. However, in the present study, the antibacterial effect was observed in dark; hence raising a need to investigate the role of other reactive radicals in cell depletion. The free-radicals generated during the excitation of fluorescent BODIPY molecules react with surrounding cellular components and induce toxicity in living cells [29]. Such reactions being oxygen-dependent, radical species such as superoxides and hydroxyls were examined. The presence of superoxide radicals and hydroxyl radicals ($HO^{\bullet}$) was assayed by the reduction of *p*-nitrobluetetrazolium chloride (NBT) and terephthalic acid, respectively [30]. However, under these experimental conditions, the presence of such radicals was not detected. Nevertheless, $^{\bullet}OH$ has an exceedingly short lifetime; as soon as they are formed, they may react with DMSO in water to form $CH_3^{\bullet}$ and $CH_3S(OH)(O^{\bullet})$. This possibility cannot be ruled out; hence more detailed studies are required and are is underway.

In silico modeling and docking studies were performed using the Schrodinger 10.4 MacroModel [31]. The protein target for compound **3c** in *S. aureus* was retrieved from the Kyoto Encyclopedia of Genes and Genomes (KEGG) database resource and previous reports in the literature, in

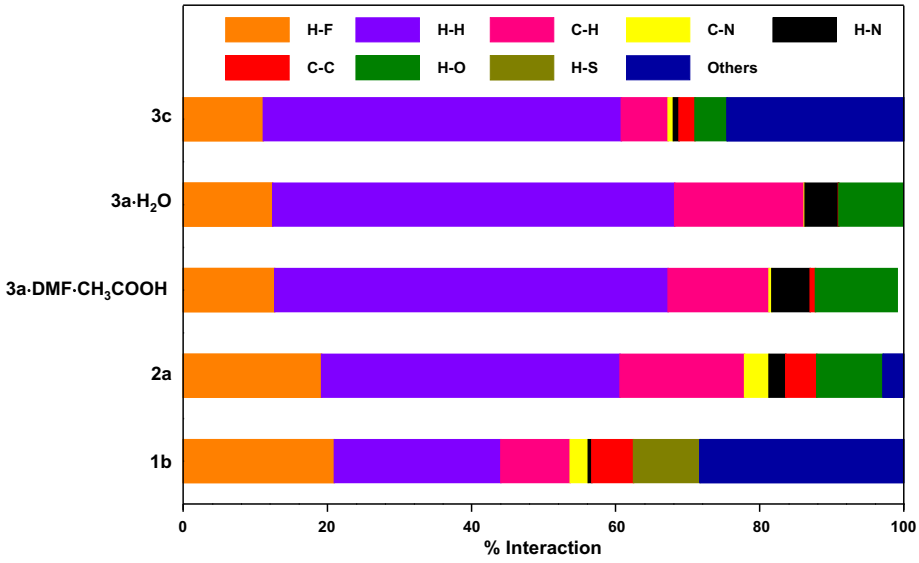

Fig. 3. Percentage contribution of various interactions of compounds, **1b**, **2a**, **3a**·H_2O, **3a**·**DMF**·CH_3COOH and **3c**

Table 4. Percentage zone of inhibition, MIC and MBC values of BODIPYs against *S. aureus*

Compound	Zone of inhibition (%)		MIC (μg/mL)	MBC (μg/mL)
	Light	Dark		
1a	14.44	12.00	60	100
1b	17.78	16.11	40	80
1c	19.44	20.00	40	80
2a	13.89	12.00	80	100
2b	21.67	15.56	40	60
2c	22.22	17.78	40	60
3a	14.44	14.44	80	100
3c	18.89	15.55	20	60
Vancomycin	21.00	21.00	10	20

order to understand the mode of interaction between **3c** and target proteins in *S. aureus* as shown in Table S2. The molecule **3c** exhibited a maximum glide score of -4.89 with DNA gyrase B (Table S2). The H bond between the –NH group of **3c** and the ASP 81 residue of the enzyme was the major stabilizing interaction between the ligand and the enzyme in its active site, Figs 4a and 4b. Positively charged and polar interactions also play a role in the binding of ligand **3c** into the active site of the protein. Hydrophobic interaction from residues surrounding the ligand is yet another major main stabilizing factor for the complex.

The *in silico* results were further affirmed by *in vitro* experiments with **3c** and the purified protein. The type II topoisomerase DNA gyrase can introduce negative supercoils into DNA at the expense of ATP hydrolysis [32]. Certain antibacterials inhibit gyrase-catalyzed supercoiling of DNA by inhibiting the gyrase ATPase reaction by competing with ATP for binding to GyrB. Their binding site lies in the 24-kDa amino terminal subdomain of GyrB. The DNA gyrase inhibitory activity of **3c** was assessed in an *in vitro* supercoiling assay by gel electrophoresis [33]. It was observed that the supercoiling activity was inhibited completely by the compound even at MIC concentration, 20 μg/mL, showing that **3c** is a potent inhibitor of the enzyme *in vitro* as shown in Fig. 4c.

The BODIPY, being neutral, easily penetrates cell membranes and is likely to accumulate into subcellular membranes due to its lipophilicity. The fluorescence microscopic images shown in Fig. 5c show complete internalization of the compound inside the cells and confirm that the antimicrobial activity of the test compound **3c** against *S. aureus* is due to their efficient uptake by the bacterial cells. In addition, the morphological changes induced by **3c** on *S. aureus* was evaluated by scanning electronic microscopy (SEM) [34], as shown in Figs 5d and 5e. The images clearly showed regular well defined clustered and smooth surfaced *S. aureus* cells and no difference in morphology was observed between treated and untreated cells. Hence, it could be inferred that due to exposure of the compound **3c**, the membrane morphology of the bacterial cells is unaffected.

ADMET properties (absorption, distribution, metabolism, excretion and toxicity) evaluate the drug likeness of a molecule based on a set of *in silico* guidelines [35]. Here, ADMET predicts optimum PhysChem and oral absorption properties for the molecule 3c. The results are well in accordance with RO5, Veber and Egan rules as shown in Figs 6a and 6b and Table 5. However, according to the Pfizer rule, **3c** shows cytotoxicity in *in*

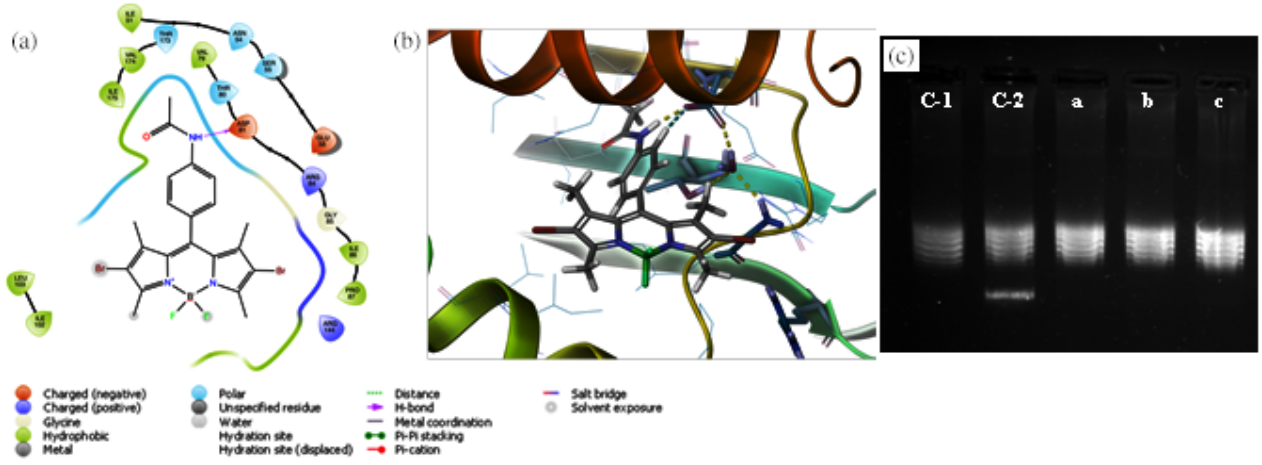

Fig. 4. (a) 2D, (b) 3D images of docking **3c** with DNA gyrase B subunit of *S. aureus* and (c) Gel Electrophoresis showing the inhibition of supercoiling activity of DNA gyrase of *S. aureus* at different concentrations of the test compound; lane C-1-negative control (relaxed DNA alone), lane C-2-positive control (relaxed DNA + enzyme), lane a–c (relaxed DNA + enzyme + different concentrations of the compound, **3c** (a) 20 (b) 40 and (c) 60 µg/mL

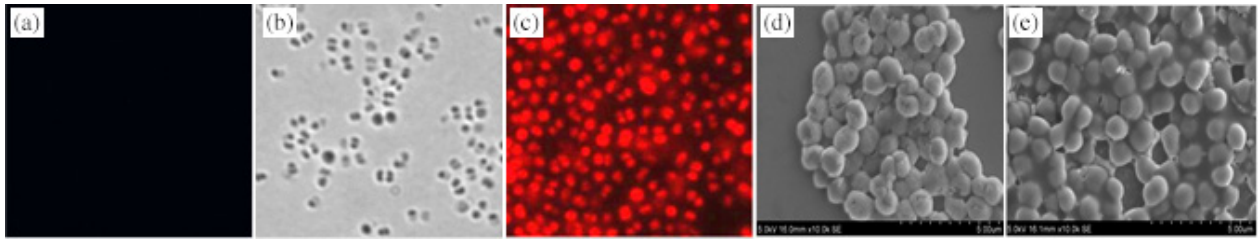

Fig. 5. Fluorescence microscopic images of bacterial cells at 100x showing the uptake of **3c** by *S. aureus* cells (a) untreated cells (b) bright field image and (c) cells treated with **3c**. Scanning electron microscopy (SEM) images of *S. aureus* (d) untreated and (e) treated with 40 µM of **3c**

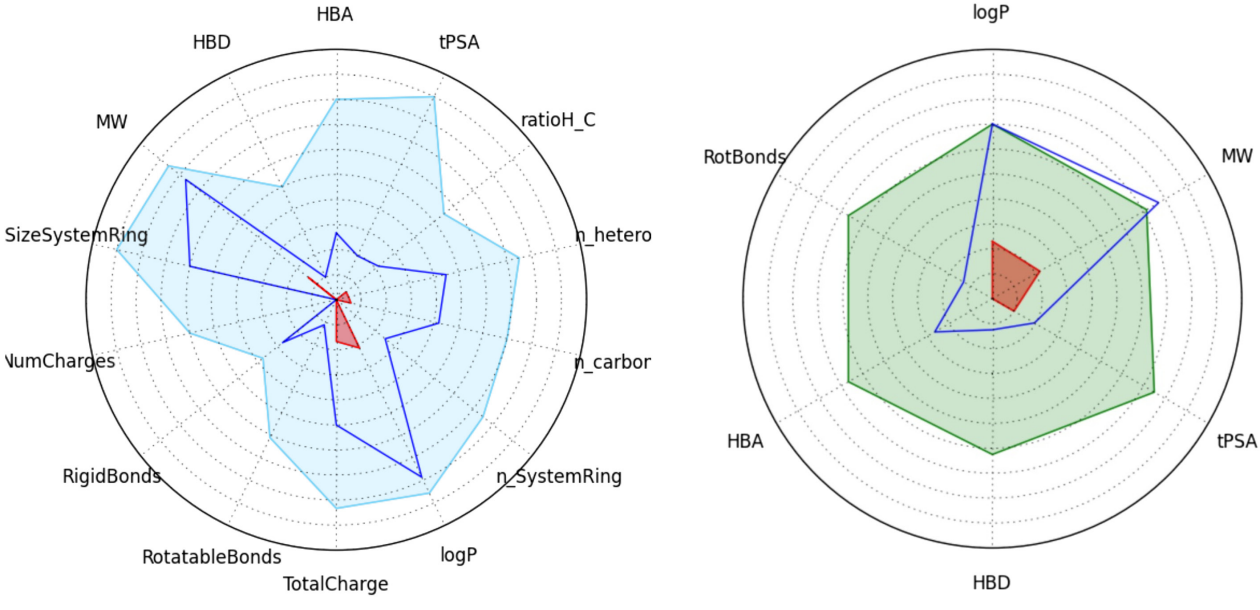

Fig. 6. (a) PhysChem filter positioning and (b) oral absorption estimation of **3c**

Table 5. The ADMET properties of BODIPY **3c**

Molecular weight	539.02 g/mol	Rigid bonds	22
[a]Log P	5.01	Flexibility	0.08
[b]Log D	-0.42	[e]HBD	1
[c]Log Sw	-6.37	[f]HBA	4
[d]tPSA	37.04	Veber rule	Good
Rotatable bond count	2	Egan rule	Good

[a]P refers to partition coefficient, logarithm of the partition coefficient between *n*-octanol and water, characterize lipophilicity. [b]D is distribution-coefficient, logD represents logP at pH 7.4. [c]logSw represents the logarithm of compound's water solubility. [d]Topological polar surface area is the sum of tabulated surface contributions of polar fragments. [e]Hydrogen bond donors and [f]acceptors.

silico analysis. Though this seems to impose a limitation on the antimicrobial application of the compound, the report on antimicrobial photodynamic therapeutic agents based upon the brominated BODIPYs affirmed the use of **3c** as antibacterial agent [28] and demanding further research on its cytotoxic effects. MTT assay was also carried out to determine the cytotoxicity of compound **3c**. The compound exhibited concentration-dependent cytotoxicity towards A549, human epithelial cell lines.

EXPERIMENTAL

Synthesis

To a solution of corresponding aldehyde (100 mg) in pyrrole (25/50 equiv.) a catalytic amount of TFA (0.1 equiv.) was added and the mixture was degassed with a stream of N_2 for 5 min. The mixture was stirred under N_2 atmosphere for 30 min at room temperature and upon completion of the reaction was quenched with dilute NaOH (0.1 M, 5 mL). The product was extracted with ethyl acetate, washed with water, dried over anhydrous Na_2SO_4 and evaporated to dryness under vacuum. The crude product was purified by silica gel column chromatography using chloroform/ hexane as the eluent to give light yellow crystalline solid.

The corresponding dipyrromethane (100 mg) was dissolved in distilled dichloromethane and was oxidized with 1 equiv. of DDQ at room temperature under stirring for 1 h. Triethylamine (30 equiv.) was added and the solution was stirred for additional 15 min. $BF_3 \cdot OEt_2$ (41 equiv.) was then added, and stirring continued at room temperature for 1 h. TLC analysis indicated the formation of the expected compound as an orange-red spot. The resulting mixture was then washed with water and extracted with CH_2Cl_2. The organic layers were then combined, dried over anhydrous Na_2SO_4, and the solvent was rotary evaporated. The resulting crude product was purified by silica gel column chromatography using chloroform/ hexane and afforded the pure compound as an orange solid in good yield. The BODIPY (100 mg) was then subjected to NBS bromination (3 equiv.) in dichloromethane at room temperature overnight. The reaction mixture was washed with water and extracted in CH_2Cl_2. The extract was dried over anhydrous Na_2SO_4, and the solvent was rotary evaporated. This was then purified by column chromatography on silica/neutral alumina gel using chloroform/hexane or chloroform/ acetone.

The BODIPYs **1a** and **2a** were dark orange powders, **3a** was green, and all appeared orange-green in organic solvents. The 2,6-di-bromo derivatives **1b** and **2b** were bright pink, both in the solid form and in solution whereas **3c** and all other 2-monobromo derivatives were pinkish orange as, shown in Fig. S22.

5-(3-*thienyl*)*dipyrromethane* (1). Yield 114 mg (56%). ^{1}H NMR (400 MHz; $CDCl_3$; Me_4Si): δ_H ppm 5.51 (1H, s, *meso*-H py), 5.95 (2H, s, py), 6.15 (2H, m, py), 6.65 (2H, d, thio), 6.96 (2H, d, thio), 7.28 (1H, m, thio), 7.86 (2H, s, py-NH).

5-(4-*Acetamido*)*dipyrromethane* (2). The crude product was recrystallized in $CHCl_3$/hexane to afford a white solid **2**. Yield 136 mg (80%). ^{1}H NMR (400 MHz; $CDCl_3$; Me_4Si): δ_H ppm 2.14 (3H, s, -CH_3), 7.99 (2H, s, py-H), 6.68 (2H, s, py-H), 6.14 (2H, s, py-H), 5.89 (2H, s, py-H), 5.43 (1H, s, *meso* H), 7.39 (2H, d, Ar-H), 7.13 (2H, d, Ar-H).

1,3,5,7-*Tetramethyl*-5-(4-*acetamido*)*dipyrromethane* (3). The crude product was recrystallized in $CHCl_3$/ hexane to afford a reddish solid as **3** which was subjected to BODIPY synthesis without any further purification.

8-(3-*thienyl*)-4-*bora*-3*a*,4*a*-*diaza*-*s*-*indacene* (1*a*). The crude product was purified using chloroform/hexane (50/50) to afford the pure compound as an orange solid. Yield 62.mg (52%). ^{1}H NMR (400 MHz; $CDCl_3$; Me_4Si): δ_H ppm 6.55–6.56 (1H, d, py-H, ^{3}J (H, H) = 2.8 Hz), 7.11–7.10 (2H, d, py-H, ^{3}J (H, H) = 3.6 Hz), 7.39–7.38 (1H, d, ^{3}J (H, H) = 4.8 Hz), 7.53–7.51 (1H, m) 7.72 (1H, d, thio-H, J = 2 Hz), 7.92 (2H, s, py-H). IR (KBr,): ν, cm^{-1} 3110, 2918, 2669, 1626, 1545, 1394, 1377, 1351, 1363 1150, 775.

8-(4-*Acetamido*)-4-*bora*-3*a*,4*a*-*diaza*-*s*-*indacene* (2*a*). The crude product was purified by silica gel column chromatography chloroform/hexane = 95/5 to yield the pure orange fluorescent dye. Yield 79 mg (68%). ^{1}H NMR (400 MHz; $CDCl_3$; Me_4Si): δ_H ppm 2.17 (3H, s, -CH_3), 7.3 (1H, s, NH), 7.93 (2H, s, Ar-H), 7.70–7.68 (2H, d, Ar-H, ^{3}J (H, H) = 8.4 Hz), 6.55 (2H, d, py-H, ^{3}J (H, H) = 3.6 Hz), 6.95–6.96 (2H, d, py-H, ^{3}J (H, H) = 4 Hz), 7.57–7.55 (2H, d, py-H, ^{3}J (H, H) = 8.4 Hz). IR (KBr,): ν, cm^{-1} 3435, 3246, 2924, 2372, 1670, 1590, 1548, 1411, 1386, 1296, 1259, 1181, 1019, 976, 859, 831, 774.

1,3,5,7-*Tetramethyl*-8-(4-*acetamido*)-4-*bora*-3*a*,4*a*-*diaza*-*s*-*indacene* (3*a*). The crude product was purified

by silica gel column chromatography chloroform/acetone 90/10 to yield the pure orange fluorescent dye. Yield 60 mg (53%). ^{1}H NMR (400 MHz; $CDCl_3$; Me_4Si): δ_H ppm 1.25 (6H s, py-CH_3), 2.54 (6H s, py-CH_3), 2.22 (3H s, -CH_3), 5.97 (2H s, py-H), 7.66–7.68 (2H d, Ar-H, ^{3}J (H, H) = 8.4 Hz), 7.26–7.21 (2 H m, Ar-H, ^{3}J (H, H) = 8 Hz), 7.40 (1H, s, -NH). IR (KBr): ν, cm^{-1} 3585, 3339, 3042, 2922, 2851, 1541, 1468, 1402, 1371, 1083, 1054, 982, 829, 764.

2-*Bromo*-8-(3-*thienyl*)-4-*bora*-3*a*,4*a*-*diaza*-*s*-*indacene* (1*b*). The brominated derivatives were purified by column chromatography on silica gel using chloroform/hexane (50/50) as eluent and afforded the products. Yield 36 mg (30%). ^{1}H NMR (400 MHz; $CDCl_3$; Me_4Si): δ_H ppm 6.53–6.54 (1H, d, py-H, ^{3}J (H, H) = 4 Hz), 6.97 (1H, s, py-H), 7.09–7.10 (1H, d, py-H, ^{3}J (H, H) = 4 Hz), 7.29–7.31 (1H, d, thio-H, ^{3}J (H, H) = 4 Hz), 7.46–7.48 (1H, m, thio-H), 7.66–7.67 (1H, m, thio-H), 7.70 (1H, s, py-H), 7.91 (1H, s, py-H). ^{13}C NMR (400 MHz; $CDCl_3$; Me_4Si): δ_C ppm 145.8, 141.9, 142.2, 135.0, 134.0, 133.9, 132.5, 130.3, 129.8, 129.6, 127.3, 119.4, 105.8. IR (KBr): ν, cm^{-1} 3429, 3108, 2962, 2925, 1734, 1642, 1532, 1469, 1349, 1263, 1211, 845, 812, 771. HRMS (ESI-TOF): m/z 341.9475 (calcd. for $C_{13}H_8BBrF_2N_2S$ M^+ 351.97).

2,6-*Dibromo*-8-(3-*thienyl*)-4-*bora*-3*a*,4*a*-*diaza*-*s*-*indacene* (1*c*). Yield 86 mg (55%). ^{1}H NMR (400 MHz; $CDCl_3$; Me_4Si): δ_H ppm 7.05–7.01 (m, 2H, py-H), 7.75 (s, 2H, py-H), 7.26–7.30 (1H, m, thio-H), 7.48–7.50 (1H, m, thio-H,), 7.66–7.69 (1H, m, thio-H). IR (KBr): ν, cm^{-1} 3422, 3107, 2922, 2852, 1664, 1544, 1471, 1346, 1252, 997, 981, 966, 913, 848, 717, 782. HRMS (ESI-TOF): m/z 413.1855 (calcd. for $C_{13}H_7BBr_2F_2N_2S$ 431.89).

2-*Bromo*-8-(4-*acetamido*)-4-*bora*-3*a*,4*a*-*diaza*-*s*-*indacene* (2b). The brominated derivatives were separated by column chromatography on silica gel using chloroform/acetone (93.75/6.25) as eluent and afforded the products. Yield 11 mg (9%). ^{1}H NMR (400 MHz; $CDCl_3$; Me_4Si): δ_H ppm 6.50–6.51 (1H, m, py-H), 6.80 (1H, s, py-H), 6.91–6.92 (1H, d, py-H, ^{3}J (H, H) = 4.4 Hz), 7.40–7.42 (2H, d, Ar-H, ^{3}J (H, H) = 8.4 Hz), 7.63–7.65 (2H, d, Ar-H, ^{3}J (H, H) = 8.4 Hz), 7.67 (1H, s; py-H), 7.89 (1H, s, py-H), 8.00 (1H, s, NH), 2.15 (3H, s, -CH_3). ^{13}C NMR (400 MHz; $CDCl_3$; Me_4Si): δ_C ppm 210.9, 168.9, 146.6, 145.7, 141.7, 141.3, 135.1, 134.1, 133.0, 131.6, 130.1, 128.6, 119.5, 105.8, 69.7, 53.8, 31.7, 29.2, 24.5. IR (KBr): ν, cm^{-1} 3393, 3115, 2923, 2852, 2372, 2345, 1472, 1402, 1299, 1258, 1224, 1183, 758, 745. HRMS (ESI-TOF): m/z 402.0258 (calcd. for $C_{17}H_{13}BBrF_2N_3O$ $[M + 1]^+$ 403.02).

2,6-*Dibromo*-8-(4-*acetamido*)-4-*bora*-3*a*,4*a*-*diaza*-*s*-*indacene* (2c). Yield 26 mg (18%). ^{1}H NMR (400 MHz; $CDCl_3$; Me_4Si): δ_H ppm 6.89 (1H, s, py-H), 7.43–7.45 (2H, d, Ar-H, ^{3}J (H, H) = 8.4 Hz), 7.66–7.67 (2H, d, Ar-H, ^{3}J (H, H) = 7.6 Hz), 7.74 (1H, s, py-H), 7.83 (1H, s, NH), 2.17 (3H, s, -CH_3). ^{13}C NMR (400 MHz; $CDCl_3$; Me_4Si): δ_C ppm 210.8, 168.8, 146.5, 143.7, 141.5, 134.4, 131.6, 128.3, 119.5, 107.1, 69.6, 53.8, 31.7, 29.2, 24.6 IR (KBr): ν, cm^{-1} 3736, 3442, 2924, 2853, 2372, 2089, 1638, 1597, 1375, 1351, 1258, 1181, 754. HRMS (ESI-TOF): m/z 483.9463 (calcd. for $C_{17}H_{12}BBr_2F_2N_3O$ $[M–H]^+$ 482.91).

2,6-*Dibromo*-1,3,5,7-*tetramethyl*-8-(4-*Acetamido*)-4-*bora*-3*a*,4*a*-*diaza*-*s*-*indacene* (3c). The compound was isolated using neutral alumina column using chloroform/acetone (95/5). Yield 42 mg (30%). ^{1}H NMR (400 MHz; $CDCl_3$; Me_4Si): δ_H ppm 7.11–7.13 (2H, d, Ar-H, ^{3}J (H, H) = 8.4 Hz), 7.63–7.65 (2H, d, Ar-H, ^{3}J (H, H) = 8.4 Hz), 2.52 (6H, s, -CH_3), 2.16 (3H, s, -CH_3), 1.34 (6H, s, -CH_3). ^{13}C NMR (400 MHz; $CDCl_3$; Me_4Si): δ_C ppm 168.4, 154.0, 141.6, 140.5, 139.3, 130.5, 129.8, 128.6, 120.0, 111.8, 24.7, 13.6–13.9. IR (KBr): ν, cm^{-1} 3851, 3626, 2923, 2852, 1673, 1596, 1537, 1466, 1402, 1348, 1311, 1177, 1000, 763. HRMS (ESI-TOF): m/z 539.9919 (calc. for $C_{21}H_{20}BBr_2F_2N_3O$ M^+ 539.02).

CONCLUSION

In summary, we have described the synthesis and characterization of series of brominated BODIPYs; their structural, photophysical and electrochemical properties have also been explored. The biological properties of the compounds were investigated against *S. aureus* and it was found that the dibromo derivative **3c** showed better antibacterial activity with good MIC and MBC values. M molecular docking studies were performed and the target of 2,6-dibromo derivative **3c** in *S. aureus* was identified as the B subunit of DNA gyrase. *In silico* target studies were further validated by *in vitro* experiments with purified protein. Through the results obtained from the present work, it can be concluded that the brominated BODIPY **3c** should be further explored as potent antibacterial lead structure in various biomedical applications.

Acknowledgments

The Department of Science and Technology (DST), New Delhi, through EMR/2016/002396 project, is acknowledged for funding. Dr. Babu Varghese, SAIF, IIT Madras is warmly acknowledged for the single crystal data collection, structure solution and refinement. The manuscript was written through contributions of all authors. All authors have given approval to the final version of the manuscript. The authors declare no competing financial interest. It is the author's responsibility to obtain written permission to reproduce previously published material.

Supporting information

Experimental, synthetic procedure, UV-vis, fluorescence, ^{1}H, ^{13}C NMR spectra, mass spectra, electrochemical data, crystal data, images and tables are given in the supplementary material. This material is available free of charge *via* the Internet at http://www.worldscinet.com/jpp/jpp.shtml. Crystallographic data have been deposited

at the Cambridge Crystallographic Data Centre (CCDC) under numbers CCDC-1577779 (**1b**), 1022866 (**2a**), 1033432 (**3a**·H_2O) and 1058023 (**3a**·DMF·CH_3COOH) and 1577778 (**3c**). Copies can be obtained on request, free of charge, *via* http://www.ccdc.cam.ac.uk/data_request/cif or from the Cambridge Crystallographic Data Centre, 12 Union Road, Cambridge CB2 1EZ, UK (fax: +44 1223-336-033 or email: deposit@ccdc.cam.ac.uk).

REFERENCES

1. Boens N, Leen V and Dehaen W. *Chem. Soc. Rev.* 2012; **41**: 1130–1172.
2. Mendive-Tapia L, Subiros-Funosas R, Zhao C, Albericio F, Read ND, Lavilla R and Vendrell M. *Nat. Protoc.* 2017; **12**: 1588–1619.
3. Quan L, Liu S, Sun T, Guan X, Lin W, Xie Z, Huang Y, Wang Y and Jing X. *ACS Appl. Mater. Interfaces* 2014; **6**: 16166–16173.
4. Liu X, Chen B, Li X, Zhang L, Xu Y, Liu Z, Cheng Z and Zhu X. *Nanoscale* 2015; **7**: 16399–16416.
5. Raut S, Kimball J, Fudala R, Doan H, Maliwal B, Sabnis N, Lacko A, Gryczynski I, Dzyuba SV and Gryczynski Z. *Phys. Chem. Chem. Phys.* 2014; **16**: 27037–27042.
6. Peveler WJ, Noimark S, Al-Azawi H, Hwang GB, Crick CR, Allan E, Edel JB, Ivanov AP, MacRobert AJ and Parkin IP. *ACS Appl. Mater. Interfaces* 2018; **10**: 98–104.
7. Mendive-Tapia L, Zhao C, Akram AR, Preciado S, Albericio F, Lee M, Serrels A, Kielland N, Read ND, Lavilla R and Vendrell M. *Nat. Commun.* 2016; **7**: 1–9.
8. Gayathri T, Barui AK, Prashanthi S, Patra CR and Singh SP. *RSC Adv.* 2014; **4**: 47409–47413.
9. Caruso E, Banfi S, Barbieri P, Leva B and Orlandi VT. *J. Photochem. Photobiol. B Biol.* 2012; **114**: 44–51.
10. Orlandi VT, Rybtke M, Caruso E, Banfi S, Tolker-Nielsen T and Barbieri P. *Biofouling* 2014; **30**: 883–891.
11. Epelde-Elezcano N, Martínez-Martínez V, Peña-Cabrera E, Gómez-Durán CFA, Arbeloa IL and Lacombe S. *RSC Adv.* 2016; **6**: 41991–41998.
12. Kamkaew A, Lim SH, Lee HB, Kiew LV, Chung LY and Burgess K. *Chem. Soc. Rev.* 2013; **42**: 77–88.
13. Prasannan D, Raghav D, Sujatha S, Hareendrakrishna kumar H, Rathinasamy K and Arunkumar C. *RSC Adv.* 2016; **6**: 80808–80824.
14. Ronkin SM, Badia M, Bellon S, Grillot AL, Gross CH, Grossman TH, Mani N, Parsons JD, Stamos D, Trudeau M, Wei Y and Charifson PS. *Bioorganic Med. Chem. Lett.* 2010; **20**: 2828–2831.
15. Zidar N, Tomašič T, Macut H, Sirc A, Brvar M, Montalvão S, Tammela P, Ilaš J and Kikelj D. *Eur. J. Med. Chem.* 2016; **117**: 197–211.
16. Hurley KA, Santos TMA, Fensterwald MR, Rajendran M, Moore JT, Balmond EI, Blahnik BJ, Faulkner KC, Foss MH, Heinrich VA, Lammers MG, Moore LC, Reynolds GD, Shearn-Nance GP, Stearns BA, Yao ZW, Shaw JT and Weibel DB. *Med. Chem. Commun.* 2017; **8**: 942–951.
17. Liu J-J, Sun J, Fang Y-B, Yang Y-A, Jiao R-H and Zhu H-L. *Org. Biomol. Chem.* 2014; **12**: 998–1008.
18. Bax BD, Chan PF, Eggleston DS, Fosberry A, Gentry DR, Gorrec F, Giordano I, Hann MM, Hennessy A, Hibbs M, Huang J, Jones E, Jones J, Brown KK, Lewis CJ, May EW, Saunders MR, Singh O, Spitzfaden CE, Shen C, Shillings A, Theobald AJ, Wohlkonig A, Pearson ND and Gwynn MN. *Nature* 2010; **466**: 935–940.
19. Singh M, Singh SK, Gangwar M, Nath G and Singh SK. *RSC Adv.* 2014; **4**: 19013–19023.
20. Agazzi ML, Ballatore MB, Reynoso E, Quiroga ED and Durantini EN. *Eur. J. Med. Chem.* 2017; **126**: 110–121.
21. Aydın Tekdaş D, Viswanathan G, Zehra Topal S, Looi CY, Wong WF, Min Yi Tan G, Zorlu Y, Gürek AG, Lee HB and Dumoulin F. *Org. Biomol. Chem.* 2016; **14**: 2665–2670.
22. Sánchez-Arroyo AJ, Palao E, Agarrabeitia AR, Ortiz MJ and García-Fresnadillo D. *Phys. Chem. Chem. Phys.* 2017; **19**: 69–72.
23. Zhang X-F and Yang X. *J. Phys. Chem. B* 2013; **117**: 5533–5539.
24. Awuah SG and You Y. *RSC Adv.* 2012; **2**: 11169–11183.
25. Wiegand I, Hilpert K and Hancock REW. *Nat. Protoc.* 2008; **3**: 163–175.
26. Gomathi G, Srinivasan T, Velmurugan D and Gopalakrishnan R. *RSC Adv.* 2015; **5**: 44742–44748.
27. Shi G, Chen X, Wang H, Wang S, Guo X and Zhang X. *J. Antibiot.* (*Tokyo*). 2012; **65**: 229–236.
28. Frimannsson DO, Grossi M, Murtagh J, Paradisi F and Oshea DF. *J. Med. Chem.* 2010; **53**: 7337–7343.
29. Oliveira CS, Turchiello R, Kowaltowski AJ, Indig GL and Baptista MS. *Free Radic. Biol. Med.* 2011; **51**: 824–833.
30. Lakshmi Prasanna V and Vijayaraghavan R. *Langmuir* 2015; **31**: 9155–9162.
31. Simmons KJ, Chopra I and Fishwick CWG. *Nat. Rev. Microbiol.* 2010; **8**: 501–510.
32. Gjorgjieva M, Tomašič T, Barančokova M, Katsamakas S, Ilaš J, Tammela P, Mašič LP and Kikelj D. *J. Med. Chem.* 2016; **59**: 8941–8954.
33. Alt S, Mitchenall LA, Maxwell A and Heide L. *J. Antimicrob. Chemother.* 2011; **66**: 2061–2069.
34. Devi KP, Nisha SA, Sakthivel R and Pandian SK. *J. Ethnopharmacol.* 2010; **130**: 107–115.
35. Gleeson MP, Hersey A, Montanari D and Overington J. *Nat. Rev. Drug Discov.* 2011; **10**: 197–208.